

Title	Cellulose propionate/poly(N-vinyl pyrrolidone-co-vinyl acetate) blends: dependence of the miscibility on propionyl DS and copolymer composition
Author(s)	Sugimura, Kazuki; Katano, Shougo; Teramoto, Yoshikuni; Nishio, Yoshiyuki
Citation	Cellulose (2013), 20(1): 239-252
Issue Date	2013-02
URL	http://hdl.handle.net/2433/169674
Right	The final publication is available at www.springerlink.com
Type	Journal Article
Textversion	author

1 **Cellulose propionate/poly(*N*-vinyl pyrrolidone-*co*-vinyl acetate) blends: dependence of**
2 **the miscibility on propionyl DS and copolymer composition**

3

4 Kazuki Sugimura, Shougo Katano, Yoshikuni Teramoto, and Yoshiyuki Nishio*

5

6 *Division of Forest and Biomaterials Science, Graduate School of Agriculture, Kyoto*

7 *University, Sakyo-ku, Kyoto 606-8502, Japan*

8

9 *To whom correspondence should be addressed.

10 E-mail: ynishio@kais.kyoto-u.ac.jp. Tel.: +81 75 753 6250. Fax: +81 75 753 6300.

11

12 **Abstract:** Blend miscibility of cellulose propionate (CP) with synthetic copolymers
13 comprising *N*-vinyl pyrrolidone (VP) and vinyl acetate (VAc) units was examined, and a data
14 map was constructed as a function of the degree of substitution (DS) of CP and the VP
15 fraction in the copolymer component. Results of DSC and FT-IR measurements indicated
16 that the pairing of CP/P(VP-*co*-VAc) formed a miscible or immiscible blend system according
17 to the balance in effectiveness of the following factors: 1) hydrogen bonding between residual
18 hydroxyls of CP and VP carbonyls of P(VP-*co*-VAc); 2) steric hindrance of propionyl
19 side-groups to the interaction specified in 1); 3) intramolecular repulsion between the two
20 units constituting the vinyl copolymer; and, additionally, 4) structural affinity between two
21 segmental moieties involving the propionyl group and VAc unit, respectively. The factor 3
22 inducing intercomponent attraction is responsible for the appearance of a so-called
23 "miscibility window" in the miscibility map, and the factor 4 substantially expands the
24 miscible region whole, wider relative to those in the maps for the corresponding blend series
25 based on cellulose acetate and butyrate. In further refined estimation by DMA and $T_{1\rho}^H$
26 quantification in solid-state ^{13}C NMR, it was found that the miscible blends of
27 hydrogen-bonding type (using CPs of DS < 2.7) were completely homogeneous on a scale
28 within a few nanometers, whereas the polymer pairs situated in the window region (using CPs
29 of DS > 2.7) formed blends exhibiting a somewhat larger size of heterogeneity (ca. 5–20 nm).

30

31 **Keywords:** Blends; Cellulose propionate; Poly(*N*-vinyl pyrrolidone-*co*-vinyl acetate);
32 Miscibility; Scale of homogeneity

33 **Introduction**

34

35 As is well known, polymer blending is useful to improve the original physical properties of
36 one or both of the components, and also to obtain new polymeric materials exhibiting
37 wide-ranging properties and/or synergistic functions unattainable in single-component
38 materials (Ultracki 1990). This should also be applicable to the blending of cellulosics as
39 one component (Nishio 1994). Especially cellulose esters (CEs) are versatile cellulose
40 derivatives and essential for further applications in various fields including molded plastics,
41 fibers, optical films, membranes, coatings, etc., and, therefore, a number of fundamental and
42 practical blend studies of CEs have been carried out (Edgar et al. 2001; Nishio 2006).

43 In previous papers (Miyashita et al. 2002; Ohno et al. 2005; Ohno and Nishio 2006), the
44 authors' group has investigated the miscibility and intermolecular interactions for blends of
45 industrially crucial CEs, cellulose acetate (CA) and butyrate (CB), with synthetic homo- and
46 copolymers comprising *N*-vinyl pyrrolidone (VP) and/or vinyl acetate (VAc) units, i.e.,
47 poly(*N*-vinyl pyrrolidone) (PVP), poly(vinyl acetate) (PVAc), poly(*N*-vinyl
48 pyrrolidone-*co*-vinyl acetate) (P(VP-*co*-VAc)). Through thermal analysis by differential
49 scanning calorimetry (DSC), it was shown that the miscibility behaviour of the CA or
50 CB/vinyl polymer pairs (generically described as CE/P(VP-*co*-VAc)) was seriously affected
51 by the degree of substitution (DS) and the ester side-chain length of the CE component, as
52 well as by the VP fraction in the copolymer component. Two maps given in Figure 1 survey
53 the estimation result.

54

<<Figure 1 (a) & (b)>>

55 In the CA/P(VP-*co*-VAc) system (Fig. 1a), Fourier transform infrared (FT-IR) and
56 solid-state ¹³C CP/MAS NMR spectroscopy revealed that the blend miscibility was mainly
57 governed by the hydrogen-bonding interactions between the residual hydroxyls of CA and the
58 carbonyls of VP units in P(VP-*co*-VAc) and the miscible blends of this interaction type were

59 homogeneous in a few nanometers scale (Miyashita et al. 2002; Ohno et al. 2005). In the
60 CB/P(VP-*co*-VAc) system (Fig. 1b), the hydrogen-bonding interaction was suppressed in
61 frequency by steric hindrance of the bulky butyryl substituent, resulting in lowering of the
62 critical DS required for attainment of the miscibility of CE with PVP and VP-rich copolymers
63 (VP content > 65 mol%), as the critical values of 2.5 for CB and 2.8 for CA are designated in
64 Figure 1. Furthermore, unlike the situation for the CA blends, highly substituted CBs of DS
65 = 2.5–2.95 made a miscible pair with P(VP-*co*-VAc) copolymers containing ca. 30–65 mol%
66 VP residues (Ohno and Nishio 2006). This unique copolymer composition range, generally
67 termed a ‘miscibility window’, emerges as a result of indirect polymer-copolymer attraction
68 driven by strong repulsion between the VP and VAc constituents of the random copolymer.
69 More concretely, since these two monomer species having mutually repellent characters were
70 randomly combined in P(VP-*co*-VAc) by covalent bonding, the copolymers tended to form a
71 miscible monophasic system with CB (DS > 2.5) so as to reduce the strong repulsion between the
72 comonomers (Ohno and Nishio 2007). The absence of such a clear miscibility window in
73 the map for the CA/P(VP-*co*-VAc) system may be interpreted as due to a strong
74 self-association ability of highly substituted CAs of DS > ~2.8; the CAs rather crystallize in a
75 cellulose triacetate II form.

76 As an extension of the above studies, our attention was then directed to a similar
77 miscibility map for cellulose propionate (CP)/P(VP-*co*-VAc) blends; the side-chain length of
78 the CE component is just intermediate between the acetyl and butyryl substituents. Great
79 interests are how far the miscible region spreads on the map constructed as a function of the
80 DS and copolymer composition, and whether that kind of miscibility window emerges or not.
81 Thereby, we will be able to make clearer the effects of the ester side-group and residual
82 hydroxyls of CE on the blend miscibility and intermolecular interactions with the vinyl
83 polymers concerned. In addition to conventional characterizations by DSC analysis and IR
84 and NMR spectra, the homogeneity of miscible blends is evaluated in refinements of the

85 mixing scale by complementary use of dynamic mechanical analysis (DMA) and proton
86 spin-lattice relaxation time ($T_{1\rho}^H$) measurements in solid-state ^{13}C NMR spectroscopy.

87

88 **Experimental**

89

90 **Materials**

91

92 Cellulose propionate (CP) samples were synthesized from cotton cellulose with a viscosity
93 average molecular weight of 252,000 via a homogeneous reaction with acid chloride/base
94 catalyst, in a procedure similar to that used in previous studies (Kusumi et al. 2008; Nishio et
95 al. 1997). Table 1 summarizes the characterization data including DS, molecular weight, and
96 glass transition temperature (T_g) for all the CP samples used in this study. The vinyl
97 polymers employed as a mixing partner for the CPs were poly(*N*-vinyl pyrrolidone) (PVP),
98 poly(vinyl acetate) (PVAc), and poly(*N*-vinyl pyrrolidone-*co*-vinyl acetate) (P(VP-*co*-VAc)),
99 basically the same as those in the preceding papers (Miyashita et al. 2002; Ohno and Nishio
100 2006). Data of characterization for all the vinyl polymers are also listed in Table 1. As
101 shown in the table, any of the P(VP-*co*-VAc) samples exhibited a single T_g , and the T_g versus
102 copolymer composition relation was in good obedience to the Fox equation (Fox and Flory
103 1954). Thus the copolymers were all regarded as essentially random copolymer. Hereafter,
104 a CP sample with DS = x is encoded as CP $_x$, and a code P(VP $_y$ -*co*-VAc $_z$) denotes
105 P(VP-*co*-VAc) copolymer of VP:VAc = y : z (in molar ratio).

106

<<Table 1>>

107

108 **Preparation of blend samples**

109

110 CP/vinyl polymer blends were prepared in film form from mixed polymer solutions by

111 solvent evaporation, in the same manner as that adopted in the preceding works (Miyashita et
112 al. 2002; Ohno and Nishio 2006). *N,N*-Dimethylformamide was selected as a common
113 solvent and the film casting was carried out at 50 °C under reduced pressure (< 10 mmHg).
114 The as-cast samples thus obtained were further dried at 50 °C *in vacuo* for 3 days.

115 For DMA measurements, the solution-cast samples were thermally molded into a
116 flattened film ca. 0.1 mm thick by using a Toyo-Seiki hot-pressing apparatus. The hot-press
117 molding was conducted at 230 °C with an applied pressure of 15 MPa for 30 s.

118

119 Measurements

120

121 DSC thermal analysis was carried out with a Seiko DSC 6200/EXSTAR 6000 apparatus.
122 The temperature readings were calibrated with an indium standard. The calorimetry
123 measurements were conducted on ca. 5-mg samples packed in an aluminum pan under a
124 nitrogen atmosphere. Each sample was first heated from ambient temperature (~25 °C) to
125 230 °C at a scanning rate of 20 °C/min, and then immediately quenched to -50 °C at a rate of
126 80 °C/min. Following this, the second heating scan was run from -50 °C to 230 °C at a rate
127 of 20 °C/min to record stable thermograms. Thermograms presented in this paper were all
128 obtained in the second heating scan and the T_g was taken as a temperature at the midpoint of a
129 baseline shift in heat flow characterizing the glass transition.

130 FT-IR spectra were measured on thinner film samples (<20 μm thick) by using a
131 Shimadzu IRPrestige-21 spectrometer. All the spectra were recorded at 20 °C in a
132 transmission method over a wavenumber range 400–4000 cm⁻¹ with a resolution of 2 cm⁻¹
133 via accumulation of 64 scans.

134 DMA was conducted by using a Seiko DMS6100/EXSTAR6000 apparatus. Strips of
135 rectangular shape (20 × 5 mm²) cut from the molded films were used for measurements of the
136 temperature dependence of the dynamic storage modulus (E') and loss modulus (E''). The

137 measuring conditions were as follows: temperature range, -150 – 300 °C; scanning rate,
138 2 °C/min; oscillatory frequency, 10 Hz.

139 High-resolution solid-state NMR experiments were performed at 20 °C in a Varian NMR
140 system 400 MHz operated at a ^{13}C frequency of 100.6 MHz. The magic-angle spinning rate
141 was 15.0 kHz. ^{13}C CP/MAS spectra were measured with a contact time of 2 ms, and a 90°
142 pulse width of 2.9 μs was employed. In the measurements of $T_{1\rho}^{\text{H}}$, a contact time of 0.2 ms
143 was used, and a proton spin-locking time τ ranged from 0.5 to 30 ms. 2048 scans were done
144 to obtain the ^{13}C CP/MAS spectra, while 4096 scans were accumulated for the relaxation time
145 measurements. Chemical shifts of ^{13}C spectra represented in ppm were referred to
146 tetramethylsilane by using the methine carbon resonance (29.47 ppm) of adamantane crystals
147 as an external reference standard. In order to minimize any possible effect due to the
148 thermal history and/or residual solvents, each sample was heat-treated at 250 °C *in vacuo* for
149 5 min just before the measurement.

150

151 **Results and discussion**

152

153 Estimation of miscibility and intermolecular interaction

154

155 The miscibility state in the present CP/vinyl polymer system was estimated basically by T_g
156 determination in DSC; generally, if any blend sample of a given polymer/polymer pair
157 exhibits a single glass transition between the T_g s of the two component polymers and a
158 composition-dependent shift of the blend T_g is clearly observed, then the pair can be regarded
159 as a miscible one on the T_g -detection scale that is usually assumed to be less than a couple of
160 tens of nanometers (Kaplan 1976; Nishio 1994; Ultracki 1990). To examine the presence of
161 intermolecular interactions, different blend compositions of selected CP/vinyl polymer pairs
162 were subjected to FT-IR and CP/MAS NMR spectra measurements.

163

164 *CP/PVP blends*

165 When CPs of DS = 1.71–2.62 were used as a counter component to PVP, the solution-cast
166 blend films prepared at 10/90–90/10 (wt/wt) compositions were all transparent in the visual
167 inspection. By contrast, CP/PVP blends of propionyl DS = 2.72–2.93 formed a
168 comparatively cloudy film at intermediate compositions of 40–70 wt% CP content.

169 Figure 2a displays DSC thermograms obtained for CP_{2.72}/PVP blends. From reading of
170 the midpoint of the respective discontinuities in heat flow, T_g of CP_{2.72} and that of PVP were
171 evaluated as 134 °C and 177 °C, respectively. For the blend samples of 20/80–80/20
172 compositions, two independent glass transitions originating from the two components were
173 clearly detected at almost the same positions as those observed for the unblended samples.
174 This behaviour of double T_g s was also noted for CP_{2.81}/PVP and CP_{2.93}/PVP blends. Thus,
175 the CPs of DS > 2.7 are taken as immiscible with PVP.

176 <<Figure 2 (a) & (b)>>

177 Contrastively, the other six pairs of CP/PVP using propionyl DSs of <2.7 imparted a
178 miscible sign. Figure 2b exemplifies DSC thermograms of CP_{2.62}/PVP blends. T_g of CP_{2.62}
179 was determined to be 138 °C. The blends with PVP gave a single, composition-dependent
180 T_g that shifted to higher temperatures along with an increase in the PVP content; thus we can
181 conclude that the CP forms a miscible monophase with PVP. This was also the case for the
182 other CPs of DS = 1.71–2.54.

183 Figure 3 compiles FT-IR spectra obtained for blends of the miscible CP_{1.71}/PVP pair, on
184 an enlarged scale for two regions of (a) O-H and (b) C=O stretching vibrations. As shown in
185 Figure 3a, the unblended CP (top data) gave a band centering at 3,482 cm⁻¹, which can be
186 associated with a mixture of free hydroxyls and intramolecularly hydrogen-bonded OH
187 groups. For the blends, it was observed that the band peak shifted to lower wavenumber
188 positions with increasing PVP content, and, concomitantly, another absorption signal became

189 more discernible as a shoulder on the side of further lower wavenumbers, as marked by a
190 white arrow at $\sim 3,300\text{ cm}^{-1}$ in Figure 3a. This new band can be ascribed to the stretching of
191 intermolecularly hydrogen-bonded OH groups (Marchessault and Liang 1960).

192 <<Figure 3 (a) & (b)>>

193 Concerning the region of C=O stretching vibration (Fig. 3b), a $1,744\text{ cm}^{-1}$ band involved
194 in the propionyl side-group of the CP component was almost unchanged in the peak location
195 by the blending with PVP. However, a carbonyl signal of PVP, observed at $1,675\text{ cm}^{-1}$ for
196 the homopolymer, became asymmetric progressively as the CP content increased in the binary
197 mixture; consequently, the absorption band was dividable into two peaks, a larger one at
198 $\sim 1,680\text{ cm}^{-1}$ and a smaller one at $\sim 1,660\text{ cm}^{-1}$ (see data for CP-rich compositions in Fig. 3b).
199 These two split IR signals for the PVP component may be associated with the free carbonyl
200 and hydrogen-bonded carbonyl groups, respectively (Masson and Manley 1991).

201 The above observations of the frequency shift and shape variation for the specific IR
202 bands are evidently attributed to the hydrogen-bonding interaction between the residual
203 hydroxyls of the CP component and the carbonyls of the PVP component. Conversely, this
204 attractive interaction would contribute as a driving force to develop the good miscibility of the
205 CP/PVP blends, as did in the CA/PVP (Miyashita et al. 2002; Ohno et al. 2005) and CB/PVP
206 systems (Ohno and Nishio 2006). In a corroborating experiment, the immiscible CP/PVP
207 blends using highly substituted CPs of DS = 2.81 and 2.93 exhibited no systematic variation
208 of the corresponding bands in their FT-IR spectra.

209 By comprehensive comparison with the previous estimation shown in Figure 1, we
210 notice that the upper limit in DS of CP miscible with PVP, which is ~ 2.7 , is just intermediate
211 between the corresponding ones, 2.8 and 2.5, for CA and CB, respectively. This is readily
212 interpretable as due to the difference in effectiveness of the steric hindrance between the three
213 ester side-groups which can inhibit the hydrogen-bonding interaction stated above, in
214 consideration of the order of bulkiness for the acetyl, propionyl, and butyryl substituents.

215

216 *CP/PVAc blends*

217 As-cast films of CP/PVAc blends were mostly transparent to the naked eye (i.e., optically
218 compatible) over the whole composition range. However, taking account of the refractive
219 index 1.47–1.49 of CP, close to that of PVAc (1.4665 (Seferis 1999)), we should note that the
220 transparency of these films is not directly linked to the blend miscibility.

221 Figure 4 collects T_g versus composition plots for eight series of CP/PVAc blends
222 (propionyl DS = 1.90–2.93). As can be seen from the plots, the three blend series using CPs
223 of DS = 1.90, 2.18, and 2.35 were completely immiscible, because two T_g signals appeared
224 without any noticeable shift from their original locations for the two components. Regarding
225 the other blend series using CPs of DS > 2.5, however, an appreciable extent of T_g shift was
226 detected for both of the two components at compositions of CP/PVAc = 60/40–90/10,
227 indicating that a certain amount of the CP constituent was dissolved into the PVAc phase, and
228 *vice versa*. Therefore, we judge the CP(DS > 2.5)/PVAc pairs to be partially miscible.
229 Such partial miscibility was never definable to the CA/PVAc and CB/PVAc systems
230 irrespective of DS of the CA or CB component; any blend of both systems provided two
231 invariable T_g s independent of the mixing composition.

232

<<Figure 4>>

233 The finding of the partial miscibility (or better compatibility) for the pairs of highly
234 propionylated CP/PVAc is quite significant in the present study, as embodied below for CP
235 blends with the copolymer P(VP-*co*-VAc). A structural affinity between the propionyl
236 side-group ($\text{CH}_3\text{-CH}_2\text{-CO-O-C-}$) and the VAc unit ($\text{-(CH}_2\text{-CH(O-CO-CH}_3\text{))-$) might be
237 responsible to the advent of the partial miscibility, as we have pointed out a similar effect in
238 former studies on CE/poly(ϵ -caprolactone) blends (Nishio et al. 1997; Kusumi et al. 2008).
239 The two structural unities containing a carbonyl moiety may be favorable for a relatively
240 weak interaction of dipole-dipole antiparallel alignment. The presence of such a weak

241 interaction is also suggested in earlier papers dealing with a miscible system of PVAc with
242 poly(methyl acrylate) ($-(\underline{\text{C}}\text{H}_2-\underline{\text{C}}\text{H}(\underline{\text{C}}\text{O}-\underline{\text{O}}-\underline{\text{C}}\text{H}_3))_n-$) (Nandi et al. 1985; Takegoshi et al. 1993).

243

244 *CP/P(VP-co-VAc) blends*

245 In visual appearance, as-cast films of CP blends with VP-VAc copolymers were homogeneous
246 and transparent, except for films of several polymer pairs composed of CP of DS > 2.7 and
247 P(VP-co-VAc) having more than 70 mol% VP residues.

248 Figure 5 displays T_g variations with mixing composition for eight series of
249 CP_{1.90}/P(VP-co-VAc) blends, the VP fraction of the copolymer component ranging from 10 to
250 87 mol%. In the data plotting, when the VP fraction in P(VP-co-VAc) was ≥ 23 mol%, any
251 blend series of CP_{1.90}/P(VP-co-VAc) provided a smooth variation of a single T_g situated
252 between the T_g values of the two unblended components. Thus, it turns out that CP_{1.90} forms
253 a miscible monophase with P(VP-co-VAc)s of VP > ~20 mol%. For selected blends of the
254 miscible pairs, the presence of the hydrogen-bonding interaction between the CP-hydroxyl
255 and VP-carbonyl groups was also ascertained by FT-IR measurements. With regard to a
256 series of CP_{1.90}/P(VP_{0.10}-co-VAc_{0.90}), a few samples of 60–80 wt% CP content gave two
257 discrete T_g s, yet there occurred a noticeable extent of T_g shift over all the blend compositions,
258 as can be seen from Figure 5. Therefore, exceptionally, this polymer pair is evaluated to be
259 partially miscible.

260

<<Figure 5>>

261 In the same way, CP_{2.18} showed a similar miscibility behaviour to that of CP_{1.90}; viz., the
262 CP was partially miscible with P(VP_{0.10}-co-VAc_{0.90}) and completely miscible with the other
263 copolymers of VP:VAc = 23:77–87:13. Intriguingly, CP_{2.35}, CP_{2.54}, and CP_{2.62} were all
264 completely miscible even with P(VP_{0.10}-co-VAc_{0.90}) as well as with the others of VP > 20
265 mol%.

266 When the propionyl DS of the CP component reached 2.72 and more, the CPs were

267 miscible with P(VP-*co*-VAc)s of ca. 10–65 mol% VP residues, despite their imperfect
268 miscibility with PVAc and PVP homopolymers. Figure 6 exemplifies the miscible evidence
269 in DSC for CP_{2.89}/P(VP_{0.52-*co*}-VAc_{0.48}) and CP_{2.89}/P(VP_{0.10-*co*}-VAc_{0.90}) combinations.
270 Accordingly, it follows that the CP/P(VP-*co*-VAc) system exhibited a definite miscibility
271 window, as did the previous CB/P(VP-*co*-VAc) system (see Fig. 1b). As for the miscibility
272 window of the latter system, it was reasonably concluded that a greater repulsion between the
273 VP and VAc units in the random copolymer was mainly contributory to the miscibility
274 attainment; this was rationalized by assessment of the Krigbaum-Wall interaction parameters
275 (Ohno and Nishio 2007). The intramolecular copolymer effect may also be applicable to the
276 present CP(DS > 2.7)/P(VP-*co*-VAc) blends.

277 <<Figure 6 (a) & (b)>>

278 It should be stressed here that the CPs of DS > 2.7 were miscible with
279 P(VP_{0.10-*co*}-VAc_{0.90}) abundant in VAc residues, as was the case for the ones of DS =
280 2.35–2.62. At the comonomer ratio of VP:VAc = 10:90, the intramolecular repulsion effect
281 would decline to a considerable extent; instead, however, the interaction coming from the
282 structural affinity between the ester side-group of CP and the VAc unit of the copolymer
283 would be more prevailing. It can therefore be assumed that, as a result of favorable balance
284 of the two effects, the high-substituted CPs were miscible with P(VP_{0.10-*co*}-VAc_{0.90}). To find
285 a spectroscopic evidence of the latter interaction in which both CP- and VAc-carbonyls should
286 be involved, we carried out FT-IR and solid-state ¹³C CP/MAS NMR measurements for
287 CP_{2.89}/P(VP_{0.10-*co*}-VAc_{0.90}) and CP_{2.89}/P(VP_{0.52-*co*}-VAc_{0.48}) blends. In the IR examination,
288 however, the C=O stretching band of CP overlapped completely with the one of VAc. In the
289 CP-MAS spectra measurements, the unblended copolymers gave a carbonyl resonance signal
290 composed of two splitting peaks with their maximum at 171 ppm (for VAc unit) and 175 ppm
291 (for VP unit); the splitting was relatively clear in a data for P(VP_{0.52-*co*}-VAc_{0.48}) (see Fig. 9).
292 Nevertheless, when the carbonyl carbon resonance of CP (173.5 ppm) merged with the split

293 signal of the VP/VAc units, it was difficult to precisely estimate the respective three chemical
294 shifts. Thus the structural affinity effect was undetectable for any of the blends; it appears to
295 be substantially feeble, however.

296 On the basis of the thermal analysis data, we successfully constructed a miscibility map
297 for the CP/P(VP-*co*-VAc) system, as shown in Figure 7. The diagram indicates that CPs of
298 $DS < 2.7$, having a relatively higher amount of residual OH groups, are mostly miscible with
299 the vinyl polymers of VP $> \sim 20$ mol%, primarily due to predominance of the
300 hydrogen-bonding interaction. A miscibility window emerges in the region satisfying
301 propionyl $DS > 2.7$ and VP fraction = 10–65 mol%, as a result of indirect intercomponent
302 attraction due to the stronger repulsion effect in the P(VP-*co*-VAc) component itself. To
303 make a comparison of the map with the previous ones (Fig. 1) for the corresponding blend
304 systems of CA and CB, we find that the CP system produced the largest miscible region. As
305 compared with the map for the CB blends, the DS boundary partitioning the miscibility states
306 of CP/P(VP-*co*-VAc) (VP ≥ 65 mol%) pairs is driven up to ~ 2.7 from the value ~ 2.5 for the
307 CB system. This elevation in DS may be ascribed to the modest effectiveness in steric
308 hindrance of the propionyl group of medium size, relative to that of the more bulky butyryl
309 group. Another factor expanding the miscible region in the map for the CP system is an
310 intermolecular accessibility derived from the structural affinity of the propionyl side-group
311 with the VAc unit; this effect may be applicable to the blending pairs of CPs of $DS > \sim 2.3$ and
312 P(VP-*co*-VAc)s of VP = ca. 10–20 mol%.

313 <<Figure 7>>

314

315 Insight into the scale of homogeneous mixing

316

317 In the previous study on the CB/P(VP-*co*-VAc) system (Ohno and Nishio 2006), it was
318 suggested that the degree of homogeneity for the combinations situated in the miscibility

319 window was somewhat lower than that for the hydrogen-bonding type of miscible blends,
320 reflecting a difference in absolute strength between the driving forces for the respective
321 miscibility attainments. In this connection, we should remark that DSC thermograms for the
322 60/40–90/10 compositions of CP_{2.89}/P(VP_{0.10-co}-VAc_{0.90}) blends exhibited a single, but
323 relatively broader glass transition (see Fig. 6b). A similar phenomenon was noted for other
324 CP/P(VP-*co*-VAc) blends satisfying DS > 2.7 for the CP and VP = 10–33 mol% for the
325 copolymer. Such a broadening in temperature range of the glass transition may be
326 interpretable as due to mixing of plural microdomains with subtly different fluctuations in
327 polymer composition (Lodge and McLeish 2000). In relation to this assumption, further
328 investigations were made into the homogeneity of mixing for the CP/P(VP-*co*-VAc) system
329 by means of DMA and nuclear magnetic relaxation measurements.

330

331 *Thermal transition behavior evaluated by DMA*

332 As far as detection of T_g is concerned, DMA is more sensitive than calorimetric measurements
333 in many cases of studies on multicomponent polymeric materials (Kusumi et al. 2011;
334 MacKnight et al. 1978; Ultracki 1990). As a conventional matter, if DSC analysis is
335 sensitive to heterogeneities with sizes of ca. 20–30 nm as an upper limit, DMA can detect a
336 somewhat finer scale of heterogeneity, e.g., a domain size smaller than ~15 nm (Kaplan 1976;
337 Masson and Manley 1991; Nishio 1994).

338 Figure 8a shows the temperature dependence of the dynamic storage modulus E' and
339 loss modulus E'' for CP_{2.89}/P(VP_{0.10-co}-VAc_{0.90}) blends of 25/75, 50/50, and 75/25
340 compositions, together with the corresponding data for plain CP_{2.89}. As for the copolymer
341 *per se*, the data was not obtained because of a brittle nature of the film. As demonstrated
342 clearly in the figure, the unblended CP_{2.89} sample showed a very sharp transition with an E''
343 peak maximum at 137 °C; this temperature is somewhat higher than T_g (127 °C) determined
344 by DSC, however. In contrast, the blend samples gave a much broader E'' peak with a low

345 onset point (~50 °C in common), and a more gradual E' falling as well, in the glass transition
346 temperature region, this trend being particularly prominent in the data for the 75/25 and 50/50
347 compositions.

348 <<Figure 8 (a) & (b)>>

349 Figure 8b compiles DMA data of CP_{2.18}/PVP and CP_{2.89}/P(VP_{0.52-co}-VAc_{0.48}) blends, the
350 illustration for each series being restricted to a few samples rich in CP content, there. Any of
351 the two blend series provided a single and sharp transition signal, both in the E'' peak and in
352 the E' drop, which shifted systematically with polymer composition. From comparison with
353 these data, the pair of CP_{2.89}/P(VP_{0.10-co}-VAc_{0.90}) described on ahead is obviously inferior in
354 the degree of miscibility to the other two, within a scale (~15 nm) detectable by DMA.
355 Incidentally, it is interesting to find a homogeneity on the DMA scale for the CP_{2.89} blends
356 with P(VP_{0.52-co}-VAc_{0.48}) having equimolar amounts of VP and VAc units, although the
357 blending pair is not of the hydrogen-bonding type such as the CP_{2.18}/PVP one but situated in
358 the miscibility window of that map (Fig. 7).

359

360 *Homogeneity estimated by solid-state ¹³C NMR relaxation*

361 As a useful technique in solid-state ¹³C NMR, $T_{1\rho}^H$ measurements for specific carbons in a
362 multicomponent polymer system make it possible to estimate the mixing homogeneity in a
363 scale of ¹H spin-diffusion length that is usually within several nanometers (Masson and
364 Manley 1991; Ohno et al. 2005; Zhang et al. 1992). $T_{1\rho}^H$ values can be obtained by fitting
365 the decaying carbon resonance intensity to the following exponential equation:

366
$$M(\tau) = M(0) \exp(-\tau/T_{1\rho}^H) \quad (1)$$

367 where $M(\tau)$ is the magnetization intensity observed as a function of the spin-locking time τ .

368 In a general rule, if two constituent polymers are in a homogeneously mixed state on the scale
369 over which ¹H spin-diffusion can take place in a time $T_{1\rho}^H$, the $T_{1\rho}^H$ values for different
370 protons belonging to the respective components may be equalized to each other by the spin

371 diffusion.

372 In terms of the NMR technique, a comparative assessment of the polymer-polymer
373 mixing scale was made for three selected series of blends, CP_{2.89}/P(VP_{0.52-co}-VAc_{0.48}),
374 CP_{1.71}/P(VP_{0.52-co}-VAc_{0.48}), and CP_{1.71}/PVP. Figure 9 exemplifies ¹³C CP/MAS spectra
375 obtained for CP_{2.89}, P(VP_{0.52-co}-VAc_{0.48}), and their 50/50 blend. The peak assignments of
376 the spectra are based on literature data for CP (Tezuka and Tsuchiya 1995), PVP (Zhang et al.
377 1992), and PVAc (Cheung et al. 2000). The experiment of $T_{1\rho}^H$ quantifications was done
378 through monitoring the following ¹³C resonance signals with better resolution: C2/C3/C5
379 pyranose carbons (74 ppm) and propionyl carbons C8 (28 ppm) and C9 (9.3 ppm) for the CP
380 component, and C_b/C_c (42 ppm) and C_δ/C_d carbons (~20 ppm) for the P(VP-co-VAc)
381 component. Figure 10a illustrates the decay behaviour in intensity of the C2/C3/C5 and
382 C_b/C_c peaks for unblended CP_{2.89} and P(VP_{0.52-co}-VAc_{0.48}), respectively, and for their 50/50
383 blend imparting both resonance signals as well. The slope of each semi-logarithmic plot
384 corresponds to an inverse of $T_{1\rho}^H$ as the time constant of the relaxation process. We found
385 from these plots that $T_{1\rho}^H$ of CP_{2.89} (18.5 ms) increased to 22.7 ms and that of
386 P(VP_{0.52-co}-VAc_{0.48}) (35.4 ms) decreased to 33.1 ms by the 50/50 blending, but they never
387 became so close to each other. Regarding the CP_{1.71}/P(VP_{0.52-co}-VAc_{0.48}) pair (Fig. 10b), on
388 the contrary, $T_{1\rho}^H$ values of the two components for the 50/50 blend coincided with each other
389 just at the midpoint (27.9 ms) between the respective original values, 20.5 ms for CP_{1.71} and
390 35.4 ms for the copolymer. A similar tendency of $T_{1\rho}^H$ variations was observed in tracing of
391 another set of the C8 or C9 signal of CP and the C_δ/C_d signal of P(VP-co-VAc).

392 <<Figure 9>>

393 <<Figure 10 (a) & (b)>>

394 Table 2 lists all the $T_{1\rho}^H$ data obtained for CP_{1.71}, CP_{2.89}, PVP, P(VP_{0.52-co}-VAc_{0.48}), and
395 their miscible blends of CP/vinyl polymer = 75/25–25/75. In the CP_{1.71}/P(VP_{0.52-co}-VAc_{0.48})
396 series, $T_{1\rho}^H$ of the CP_{1.71} component, originally 20.0 ms as an average, rises systematically

397 with an increase in the copolymer content, while that of the P(VP_{0.52-co}-VAc_{0.48}) component,
398 originally 35.0 ms as an average, diminishes correspondingly with increasing CP_{1.71} content.
399 In consequence, the two $T_{1\rho}^H$ s at every blend composition are surely in good agreement with
400 each other. Such a composition-dependent shift of the almost equalized $T_{1\rho}^H$ s of two
401 components is also observed for the CP_{1.71}/PVP blend series. Thus, it is reasonably deduced
402 that the two constituent polymers in the two series of blends are intimately mixed within a
403 range where the mutual ¹H-spin diffusion is permitted over a period of the respective
404 homogenized $T_{1\rho}^H$, e.g., ~30.5 ms for the 50/50 composition of CP_{1.71}/PVP.

405 <<Table 2>>

406 An effective path length L of the spin diffusion in a time $T_{1\rho}^H$ is given by the following
407 equation (McBrierty and Douglass 1981):

$$408 \quad L \cong (6DT_{1\rho}^H)^{1/2} \quad (2)$$

409 where D is the spin-diffusion coefficient, usually taken to be $\sim 1.0 \times 10^{-12}$ cm²/s in organic
410 polymer materials. By adopting $T_{1\rho}^H$ data of 23–31 ms approximated for the
411 CP_{1.71}/P(VP_{0.52-co}-VAc_{0.48}) blends of 75/25–25/75 compositions, the diffusion path length is
412 calculated as $L = 3.7$ – 4.3 nm. In a similar manner, L is determined to be 3.9–4.4 nm with
413 $T_{1\rho}^H = 25$ – 33 ms for the corresponding CP_{1.71}/PVP compositions. Accordingly, it is
414 confirmed that any of these miscible blends using a low-substituted CP is virtually
415 homogeneous in a scale of ca. 4 nm.

416 With regard to the CP_{2.89}/P(VP_{0.52-co}-VAc_{0.48}) series, as evidenced in Table 2, there
417 arises a serious disagreement between $T_{1\rho}^H$ s of the two polymer components at every blend
418 composition, although the mutual approach to a small extent is admitted. This larger
419 temporal disagreement implies that the relaxation processes of the two polymers in the blends
420 proceeded rather independently without their cooperative spin diffusion. By the combined
421 use of this result and the previous DMA one, it can be concluded that the scale of
422 homogeneity in the CP_{2.89}/P(VP_{0.52-co}-VAc_{0.48}) blends lies between approximately 5 and 15

423 nm.

424

425 **Conclusions**

426

427 Miscibility characterization was performed on blends of cellulose propionate (CP) with
428 synthetic vinyl polymers containing *N*-vinyl pyrrolidone (VP) and/or vinyl acetate (VAc) units,
429 i.e., PVP, PVAc, and P(VP-*co*-VAc) random copolymers. On the basis of T_g analysis by
430 DSC, a miscibility map (Fig. 7) was successfully constructed as a function of both the
431 propionyl DS of CP and the VP:VAc composition of P(VP-*co*-VAc). FT-IR spectroscopy
432 was also utilized to detect a hydrogen-bonding type of intermolecular interaction contributory
433 to the miscibility attainment. As denoted in that map, polymer pairs of CP/P(VP-*co*-VAc)
434 satisfying $DS < 2.7$ for the CP component and $VP > 20$ mol% for the vinyl polymer
435 component were miscible. This miscibility is given rise to, more or less, by virtue of the
436 hydrogen bonding between CP-hydroxyls and VP-carbonyls, and hence the effectiveness
437 should be greater when the propionyl DS is lower and the VP fraction is higher. The upper
438 limit of $DS = 2.7$ required for the miscibility was intermediate between the corresponding
439 ones, acetyl $DS = 2.8$ and butyryl $DS = 2.5$, for the comparable systems employing cellulose
440 acetate (CA) and butyrate (CB). This observation can be explained as being due to the
441 difference in bulkiness between the three sorts of acyl substituents, each exerting an effect of
442 steric hindrance to decline the hydrogen-bonding interaction.

443 CPs of $DS > 2.7$ exhibited miscibility with P(VP-*co*-VAc)s of $VP = 10\text{--}65$ mol%,
444 despite their imperfect miscibility with both PVP and PVAc homopolymers; this resulted in
445 advent of a definite 'miscibility window' in the map, as has been experienced formerly in our
446 study of CB/P(VP-*co*-VAc) blends. The behaviour may be interpreted to be occasioned
447 principally by intramolecular repulsion between the comonomer units in P(VP-*co*-VAc). In
448 addition, another effect, the structural affinity between the propionyl side-group and the VAc

449 unit, contributes to the miscibility realized for blends of highly propionylated CPs ($DS > 2.3$)
450 with VAc-rich copolymers (VP:VAc = 10:90–33:67). Eventually, the miscible pairing region
451 extended more widely in the map for the CP/P(VP-*co*-VAc) system, compared with the
452 situations in the corresponding blend systems using CA and CB. It is astonishing afresh to
453 find that only one difference in carbon number of the acyl substitution drastically changed the
454 miscibility behaviour of cellulose esters (CEs) with a given synthetic copolymer.

455 However, caution should be exercised to the scale of homogeneity in the
456 CP/P(VP-*co*-VAc) blends being estimated to form a miscible monophase. As a result of
457 further investigation by DMA and $T_{1\rho}^H$ quantifications in solid-state ^{13}C NMR, we had
458 awareness of the following respects: The miscible blends of hydrogen-bonding type are
459 completely homogeneous on a scale of a few nanometers (≤ 4 nm), whereas the blend series
460 situated in the miscibility window are homogeneous with a possible microdomain size
461 between ca. 5 and 15 nm. In the latter assessment, CP blends with P(VP-*co*-VAc)s
462 extremely rich in VAc (e.g., VP:VAc = 10:90) are excepted from the relevant group, their
463 miscibility being invited by a rather weak interaction due to the structural affinity effect.
464 The blends of exception can contain heterogeneous domains of ca. 15–20 nm sizes as a
465 tentative estimate.

466 From a practical standpoint, these results will contribute toward expanding the
467 opportunities of material design based on the CE family. Further studies along this line of
468 fundamental characterization are now in progress for CE blends with other vinyl copolymers,
469 in parallel with inquiries into their functionalities as optical and/or membrane materials. **In**
470 **the not too distant future, our effort will also be made to investigate an effect of**
471 **regioselectivity of the acyl substituent in CEs on their miscibility with synthetic polymers,**
472 **beyond the discussion in terms of the average DS parameter.**

473

474 **Reference**

475 Cheung MK, Wang J, Zheng S, Mi Y (2000) Miscibility of poly(epichlorohydrin)/poly(vinyl
476 acetate) blends investigated with high-resolution solid-state ^{13}C NMR. *Polymer*
477 41:1469–1474

478 Edgar KJ, Buchanan CM, Debenham JS, Rundquist PA, Seiler BD, Shelton MC, Tindall D
479 (2001) Advances in cellulose ester performance and application. *Prog Polym Sci*
480 26:1605–1688

481 Fox TG, Flory PJ (1954) The glass transition temperature and related properties of polystyrene.
482 Influence of molecular weight. *J Polym Sci* 14:315–319

483 Kaplan DS (1976) Structure-property relationships in copolymers to composites: molecular
484 interpretation of the glass transition phenomenon. *J Appl Polym Sci* 20:2615–2629

485 Kusumi R, Inoue Y, Shirakawa M, Miyashita Y, Nishio Y (2008) Cellulose alkyl
486 ester/poly(ϵ -caprolactone) blends: characterization of miscibility and crystallization
487 behaviour. *Cellulose* 15:1–16

488 Kusumi R, Teramoto Y, Nishio Y (2011) Structural characterization of
489 poly(ϵ -caprolactone)-grafted cellulose acetate and butyrate by solid-state ^{13}C NMR,
490 dynamic mechanical, and dielectric relaxation analyses. *Polymer* 52:5912–5921

491 Lodge TP, McLeish TCB (2000) Self-concentrations and effective glass transition
492 temperatures in polymer blends. *Macromolecules* 33:5278–5284

493 MacKnight WJ, Karasz FE, Fried JR (1978) Solid state transition behaviour of blends, chap. 5.
494 In: Paul DR, Newman S (eds) *Polymer blends*, vol 1. Academic Press, New York, pp
495 185–242

496 Marchessault RH, Liang CY (1960) Infrared spectra of crystalline polysaccharides. III.
497 Mercerized cellulose. *J Polym Sci* 43:71–84

498 Masson JF, Manley RS (1991) Miscible blends of cellulose and poly(vinylpyrrolidone).
499 *Macromolecules* 24:6670–6679

500 McBrierty VJ, Douglass DC (1981) Recent advances in the NMR of solid polymers. *J Polym*

501 Sci Part D 16:295–366

502 Miyashita Y, Suzuki T, Nishio Y (2002) Miscibility of cellulose acetate with vinyl polymers.
503 Cellulose 9: 215–223

504 Nandi AK, MAndal BM, Bhattacharyya SN (1985) Miscibility of poly(methyl acrylate) and
505 poly(vinyl acetate): Incompatibility in solution and thermodynamic characterization by
506 inverse gas chromatography. Macromolecules 18:1454–1460

507 Nishio Y (1994) Hyperfine composites of cellulose with synthetic polymers, chap. 5. In:
508 Gilbert RD (ed) Cellulosic polymers, blends and composites. Hanser, Munich, pp 95–113

509 Nishio Y (2006) Material functionalization of cellulose and related polysaccharides via
510 diverse microcompositions. Adv Polym Sci 205:97–151

511 Nishio Y, Matsuda K, Miyashita Y, Kimura N, Suzuki H (1997) Blends of
512 poly(ϵ -caprolactone) with cellulose alkyl esters: effect of the alkyl side-chain length and
513 degree of substitution on miscibility. Cellulose 4:131–145

514 Ohno T, Nishio Y (2006) Cellulose alkyl ester/vinyl polymer blends: effects of butyryl
515 substitution and intramolecular copolymer composition on the miscibility. Cellulose
516 13:245–259

517 Ohno T, Nishio Y (2007) Estimation of miscibility and interaction for cellulose acetate and
518 butyrate blends with *N*-vinylpyrrolidone copolymers. Macromol Chem Phys
519 208:622–634

520 Ohno T, Yoshizawa S, Miyashita Y, Nishio Y (2005) Interaction and scale of mixing in
521 cellulose acetate/poly(*N*-vinyl pyrrolidone-*co*-vinyl acetate) blends. Cellulose
522 12:281–291

523 Seferis JC (1999) Refractive indices of polymers. In: Brandrup J, Immergut EH, Grulke EA
524 (eds) Polymer Handbook, 4th edn. Wiley-Interscience, New York, pp 571–582

525 Takegoshi K, Ohya Y, Hikichi K (1993) Miscibility and inter-polymer interactions of the
526 poly(methyl acrylate)/poly(vinyl acetate) blend as studied by NMR in solution. Polym J

- 527 25:59–64
- 528 Tezuka Y, Tsuchida Y (1995) Determination of substituent distribution in cellulose acetate by
529 means of a ^{13}C NMR study on its propanoated derivative. Carbohydrate Research
530 273:83–91
- 531 Utracki LA (1990) Polymer alloys and blends: thermodynamics and rheology. Hanser,
532 Munich
- 533 Zhang XQ, Takegoshi K, Hikichi K (1992) High-resolution solid-state C-13 nuclear magnetic
534 resonance study on poly(vinyl alcohol)/poly(vinylpyrrolidone) blends. Polymer
535 33:712–717
- 536

537 **Figure Captions**

538

539 **Fig. 1** Miscibility maps for two blend systems (a) CA/P(VP-*co*-VAc) and (b)
540 CB/P(VP-*co*-VAc), quoted from previous papers (Miyashita et al. 2002; Ohno and Nishio
541 2006) in a rearranged style retaining the essence.

542

543 **Fig. 2** DSC thermograms obtained for (a) CP_{2.72}/PVP and (b) CP_{2.62}/PVP blends. Arrows
544 indicate a T_g position taken as the midpoint of a baseline shift in heat flow.

545

546 **Fig. 3** FT-IR spectra of CP_{1.71}, PVP, and their blends in the frequency regions of (a) O-H
547 and (b) C=O stretching vibrations. Solid arrows indicate a peak-top position in the
548 respective specific absorption bands, and white arrows indicate a shoulder band associated
549 with hydrogen bonding (see text for discussion).

550

551 **Fig. 4** T_g versus composition plots for eight series of CP/PVAc blends. DS of CP: ○, 1.90;
552 ●, 2.18; □, 2.35; ■, 2.54; △, 2.62; ▲, 2.72; ◇, 2.81; ◆, 2.93.

553

554 **Fig. 5** Composition dependence of T_g for eight series of CP_{1.90}/P(VP-*co*-VAc) blends.
555 VP:VAc in P(VP-*co*-VAc): ●, 10:90; ■, 23:77; ▽, 33:67; ◇, 40:60; +, 52:48; □, 62:38; △,
556 73:27; ○, 87:13.

557

558 **Fig. 6** DSC thermograms obtained for (a) CP_{2.89}/P(VP_{0.52}-*co*-VAc_{0.48}) and (b)
559 CP_{2.89}/P(VP_{0.10}-*co*-VAc_{0.90}) blends. Arrows indicate a T_g position.

560

561 **Fig. 7** Miscibility map for CP/P(VP-*co*-VAc) blends, as a function of DS of CP and VP
562 fraction in P(VP-*co*-VAc). Symbols indicate that a given pair of CP/P(VP-*co*-VAc) is

563 miscible (○), immiscible (×), or partially miscible (△).

564

565 **Fig. 8** Temperature dependence of the dynamic storage modulus E' and loss modulus E'' for

566 (a) CP_{2.89}/P(VP_{0.10-co-VAc}_{0.90}) and (b) CP_{2.18}/PVP and CP_{2.89}/P(VP_{0.52-co-VAc}_{0.48}) blends.

567

568 **Fig. 9** Solid-state ¹³C CP/MAS NMR spectra for CP_{2.89}, P(VP_{0.52-co-VAc}_{0.48}), and their

569 50/50 blend.

570

571 **Fig. 10** Semilogarithmic plots of the decay of ¹³C resonance intensities as a function of

572 spin-locking time τ , for solid films of (a) CP_{2.89}, P(VP_{0.52-co-VAc}_{0.48}), and their 50/50 blend,

573 and (b) CP_{1.71}, P(VP_{0.52-co-VAc}_{0.48}), and their 50/50 blend. The monitoring was conducted

574 for the peak intensity of C2/C3/C5 pyranose carbons of CP and that of C_b/C_c carbons of the

575 copolymer (see Fig. 9).

576

577 -----

578 In addition to the ten figures, there are two tables. See annexed sheets.

579 **Table 1** Characterization of CP and synthetic vinyl polymers used in the present study

Sample	DS ^a	M_w^b	M_n^b	M_w/M_n^b	$T_g / ^\circ\text{C}$	Source
CP	1.71	2,010,000	850,000	2.36	162	Synthesized
	1.90	1,860,000	824,000	2.26	161	Synthesized
	2.18	1,300,000	577,000	2.25	157	Synthesized
	2.35	2,210,000	925,000	2.39	153	Synthesized
	2.54	1,180,000	509,000	2.32	140	Synthesized
	2.62	979,000	359,000	2.73	138	Synthesized
	2.72	2,390,000	968,000	2.47	134	Synthesized
	2.81	1,990,000	837,000	2.38	128	Synthesized
	2.89	2,000,000	692,000	2.89	127	Synthesized
	2.93	1,250,000	525,000	2.38	124	Synthesized

Sample	VP content / mol% ^a	M_w^c	M_n^c	M_w/M_n^c	$T_g / ^\circ\text{C}$	Source
PVP	100	360,000 ^d	—	—	177	Nacalai Tesque, Inc.
P(VP-co-VAc)	87	56,500	28,000	2.02	124	Synthesized ^e
	73	52,100	25,000	2.08	111	Synthesized ^e
	62	51,600	24,400	2.11	101	Synthesized ^e
	52	28,000	5,120	5.47	89	Polyscience, Inc. ^f
	40	51,100	20,700	2.47	76	Synthesized ^e
	33	23,300	3,800	6.12	72	Polyscience, Inc. ^f
	23	59,400	26,100	2.27	55	Synthesized ^e
	10	46,500	27,700	1.68	45	Synthesized ^e
PVAc	0	90,000 ^d	—	—	41	Polyscience, Inc.

^a Determined by ¹H NMR.^b Determined by gel permeation chromatography (mobile phase, tetrahydrofuran at 40 °C) with polystyrene standards.^c Determined by gel permeation chromatography (mobile phase, 10 mM/L lithium bromide/*N,N*-dimethylformamide at 40 °C) with polystyrene standards.^d Nominal value.^e Synthesized in our laboratory by radical polymerization of two distilled monomers, VP (Aldrich Chemical Co.) and VAc (Nacalai Tesque, Inc.), in the same way as that described in a previous paper (Miyashita et al. 2002).^f Used after purification by dissolution in dichloromethane and reprecipitation into petroleum ether.

581 **Table 2** $T_{1\rho}^H$ values obtained for three series of blends, CP_{2.89}/P(VP_{0.52-co-VAc}_{0.48}),
 582 CP_{1.71}/P(VP_{0.52-co-VAc}_{0.48}), and CP_{1.71}/PVP

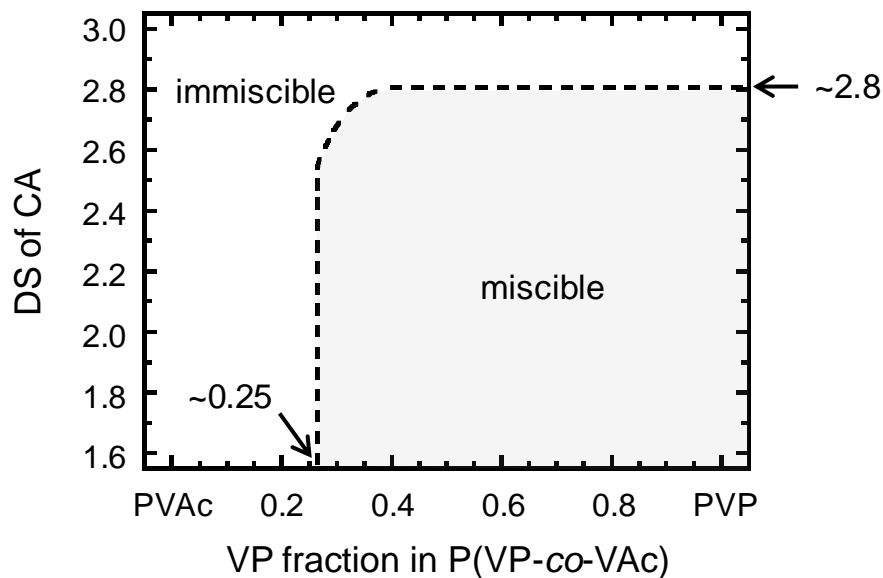
CP _{2.89} /P(VP _{0.52-co-VAc} _{0.48}) (wt/wt)	$T_{1\rho}^H$ / ms						
	CP _{2.89}				P(VP _{0.52-co-VAc} _{0.48})		
	C2/3/5	C8	C9	Ave.	b/c	δ/d	Ave.
100/0	18.5	17.6	17.7	17.9	–	–	–
75/25	20.3	18.8	18.0	19.0	32.9	29.7	31.3
50/50	22.7	20.5	19.2	20.8	33.1	30.9	32.0
25/75	25.3	22.6	21.2	23.0	34.7	33.8	34.3
0/100	–	–	–	–	35.4	34.6	35.0

CP _{1.71} /P(VP _{0.52-co-VAc} _{0.48}) (wt/wt)	$T_{1\rho}^H$ / ms						
	CP _{1.71}				P(VP _{0.52-co-VAc} _{0.48})		
	C2/3/5	C8	C9	Ave.	b/c	δ/d	Ave.
100/0	20.5	20.3	19.2	20.0	–	–	–
75/25	24.3	23.0	21.6	23.0	24.5	24.1	24.3
50/50	27.8	26.8	24.5	26.4	27.9	26.9	27.4
25/75	33.0	29.7	27.8	30.2	33.7	30.9	32.3
0/100	–	–	–	–	35.4	34.6	35.0

CP _{1.71} /PVP (wt/wt)	$T_{1\rho}^H$ / ms						
	CP _{1.71}				PVP		
	C2/3/5	C8	C9	Ave.	b/c	d	Ave.
100/0	20.5	20.3	19.2	20.0	–	–	–
75/25	25.1	24.1	23.0	24.1	26.0	26.0	26.0
50/50	30.9	30.1	30.8	30.6	30.6	29.5	30.1
25/75	33.4	33.7	33.1	33.4	33.7	33.0	33.4
0/100	–	–	–	–	32.6	31.3	32.0

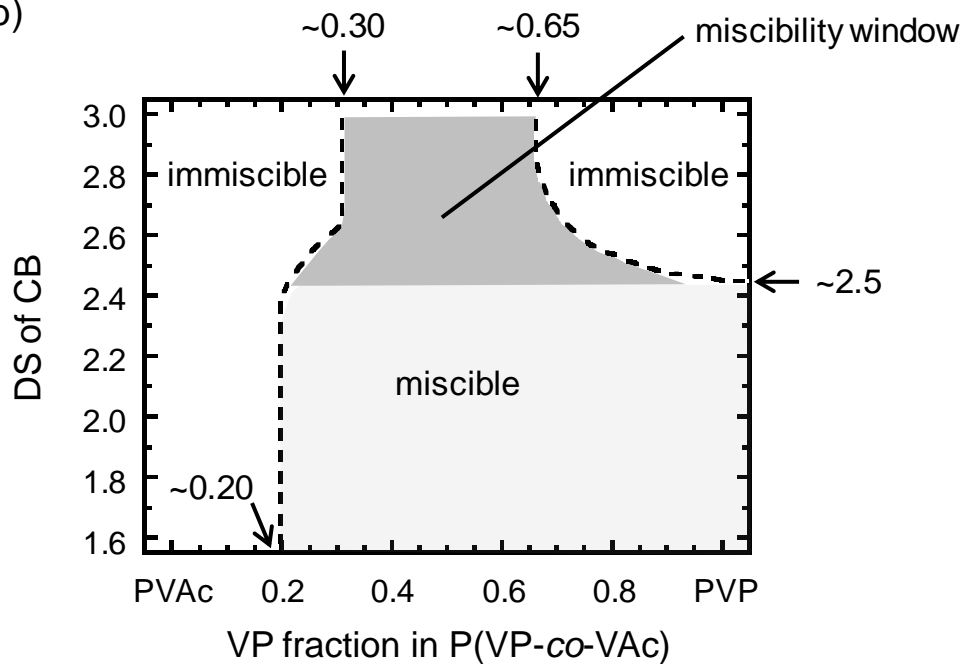
583

(a)



584

(b)

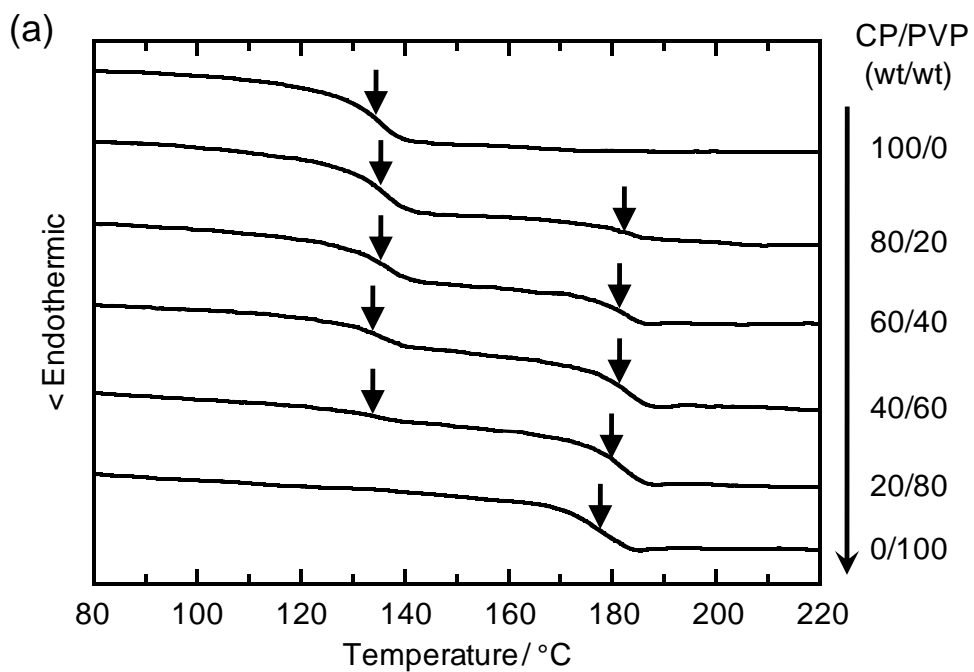


585

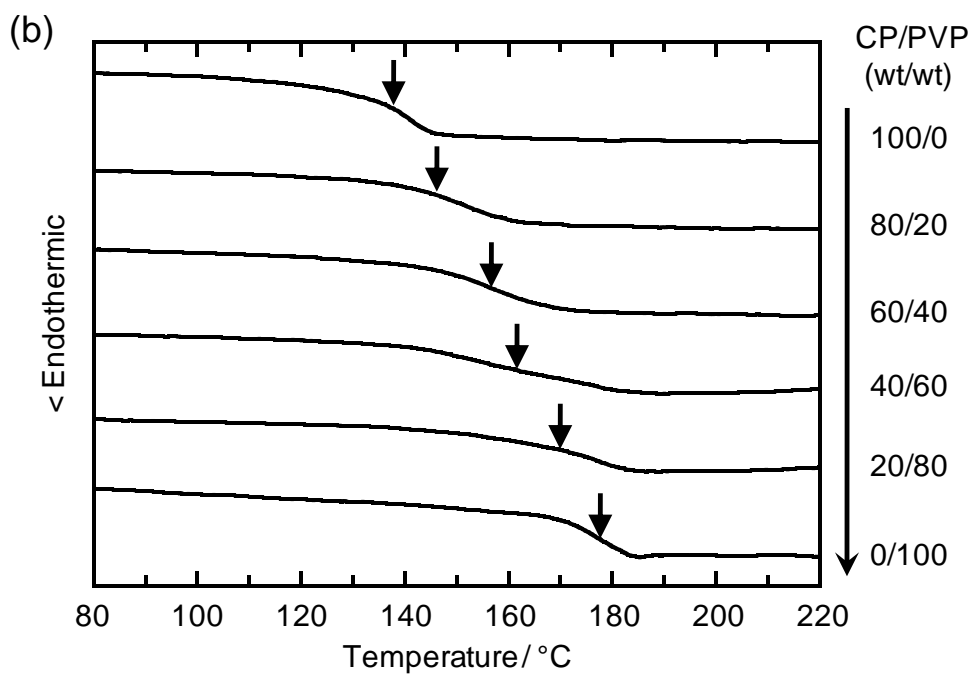
586

587 **Fig. 1** Miscibility maps for two blend systems (a) CA/P(VP-co-VAc) and (b)
588 CB/P(VP-co-VAc), quoted from previous papers (Miyashita et al. 2002; Ohno and Nishio
589 2006) in a rearranged style retaining the essence.

590



591
592

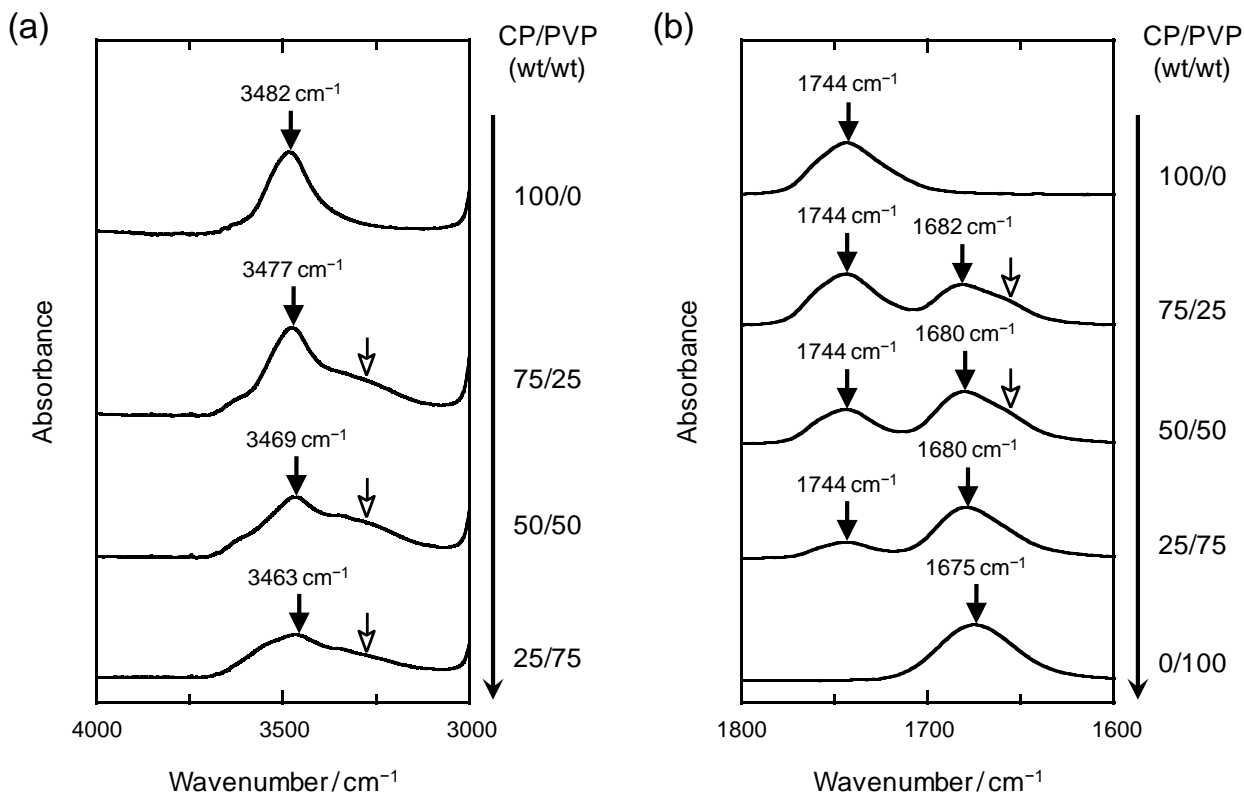


593

594

595 **Fig. 2** DSC thermograms obtained for (a) CP_{2.72}/PVP and (b) CP_{2.62}/PVP blends. Arrows
596 indicate a T_g position taken as the midpoint of a baseline shift in heat flow.

597

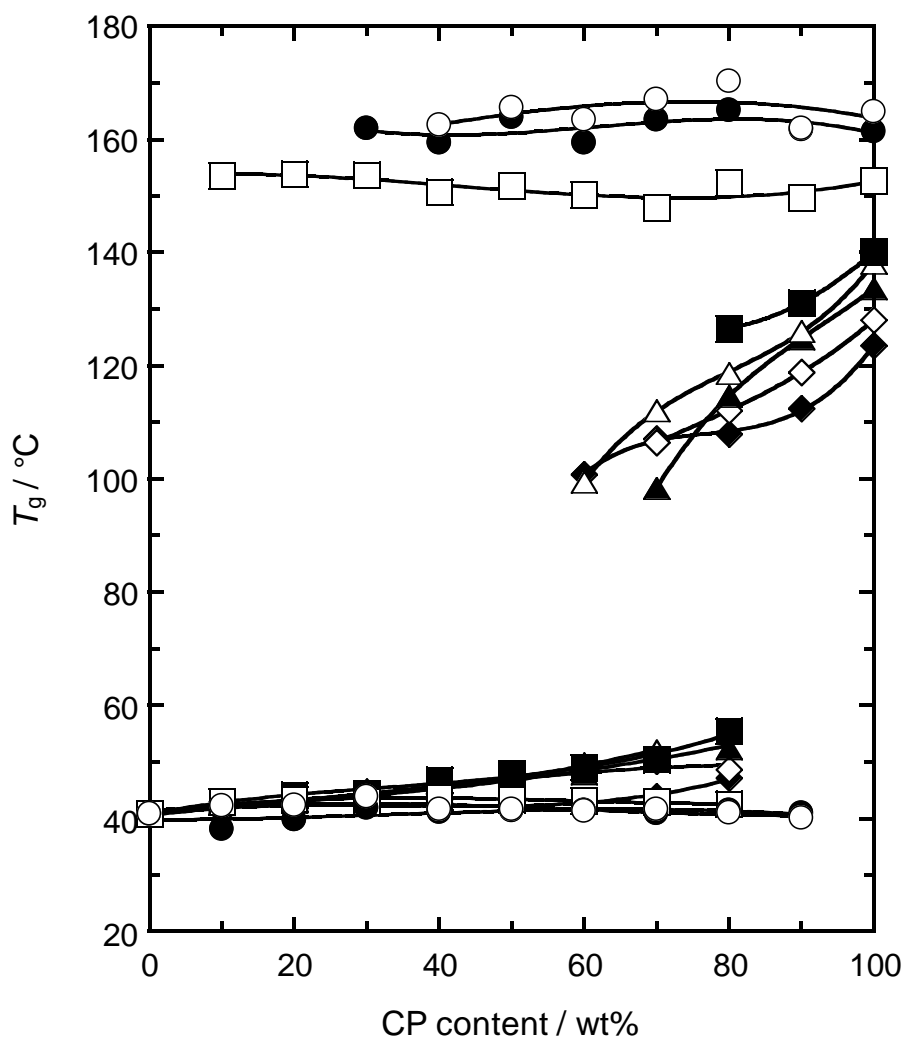


598

599

600 **Fig. 3** FT-IR spectra of CP_{1.71}, PVP, and their blends in the frequency regions of (a) O-H
 601 and (b) C=O stretching vibrations. Solid arrows indicate a peak-top position in the
 602 respective specific absorption bands, and white arrows indicate a shoulder band associated
 603 with hydrogen bonding (see text for discussion).

604



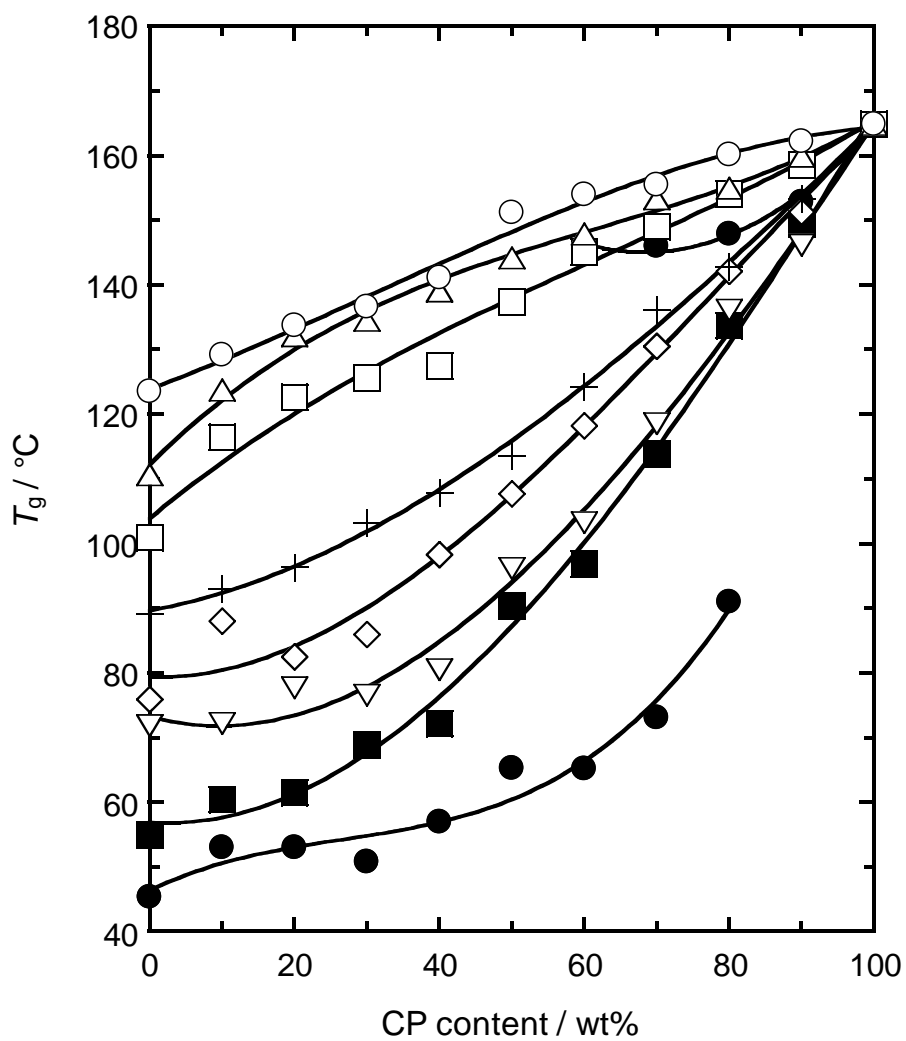
605

606

607 **Fig. 4** T_g versus composition plots for eight series of CP/PVAc blends. DS of CP: ○, 1.90;

608 ●, 2.18; □, 2.35; ■, 2.54; △, 2.62; ▲, 2.72; ◇, 2.81; ◆, 2.93.

609



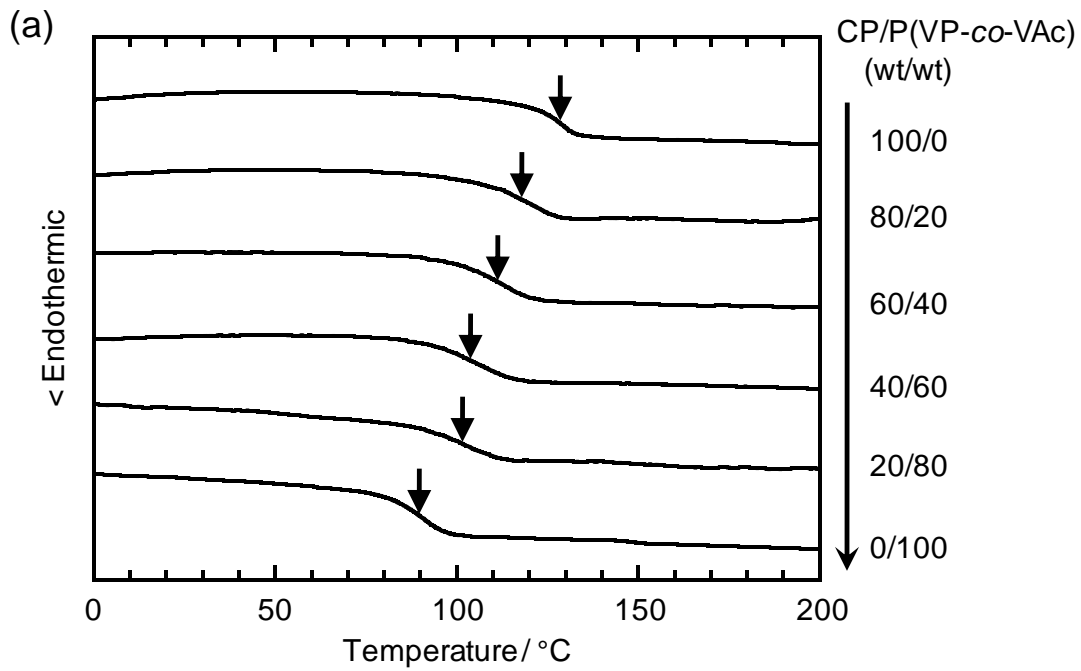
610

611

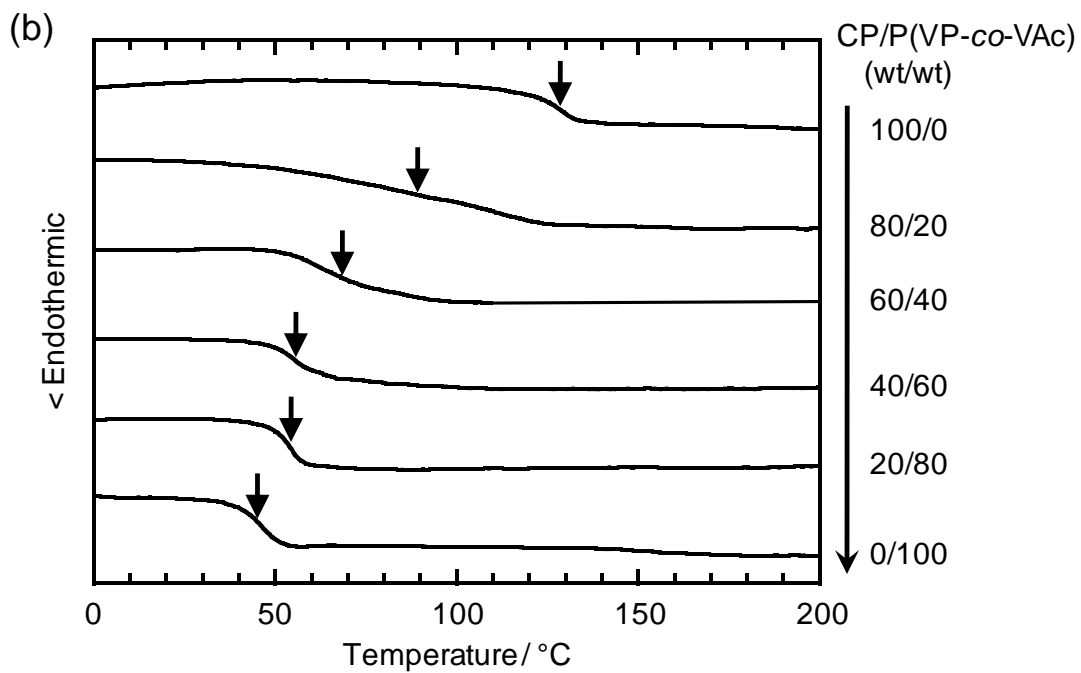
612 **Fig. 5** Composition dependence of T_g for eight series of $CP_{1.90}/P(VP-co-VAc)$ blends.

613 VP:VAc in $P(VP-co-VAc)$: ●, 10:90; ■, 23:77; ▽, 33:67; ◇, 40:60; +, 52:48; □, 62:38; △,

614 73:27; ○, 87:13.



615



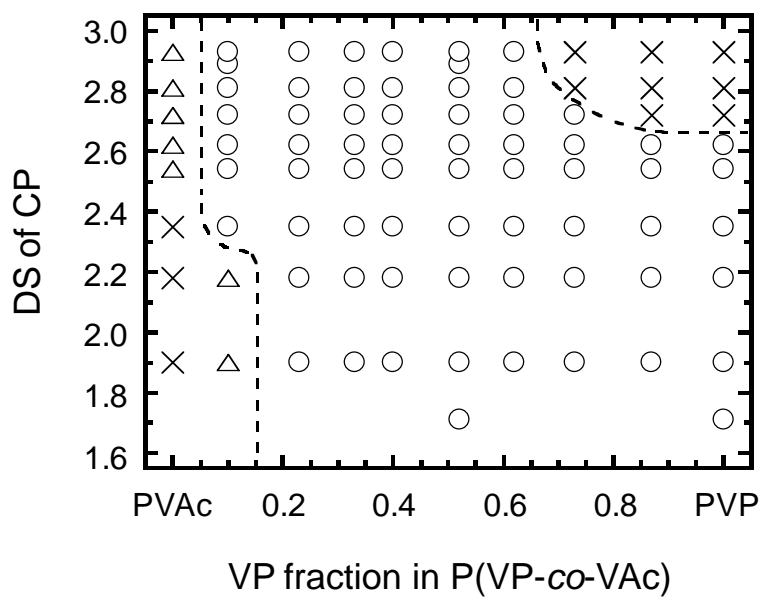
616

617

618 **Fig. 6** DSC thermograms obtained for (a) CP_{2.89}/P(VP_{0.52-co}-VAc_{0.48}) and (b)

619 CP_{2.89}/P(VP_{0.10-co}-VAc_{0.90}) blends. Arrows indicate a T_g position.

620



621

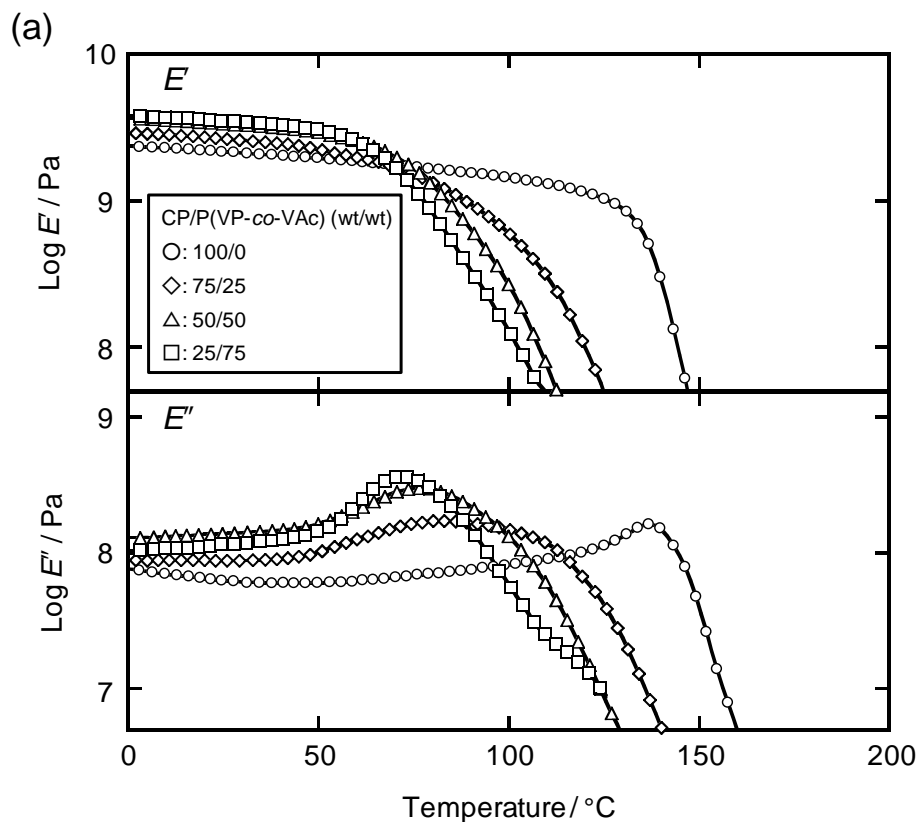
622

623 **Fig. 7** Miscibility map for CP/P(VP-co-VAc) blends, as a function of DS of CP and VP

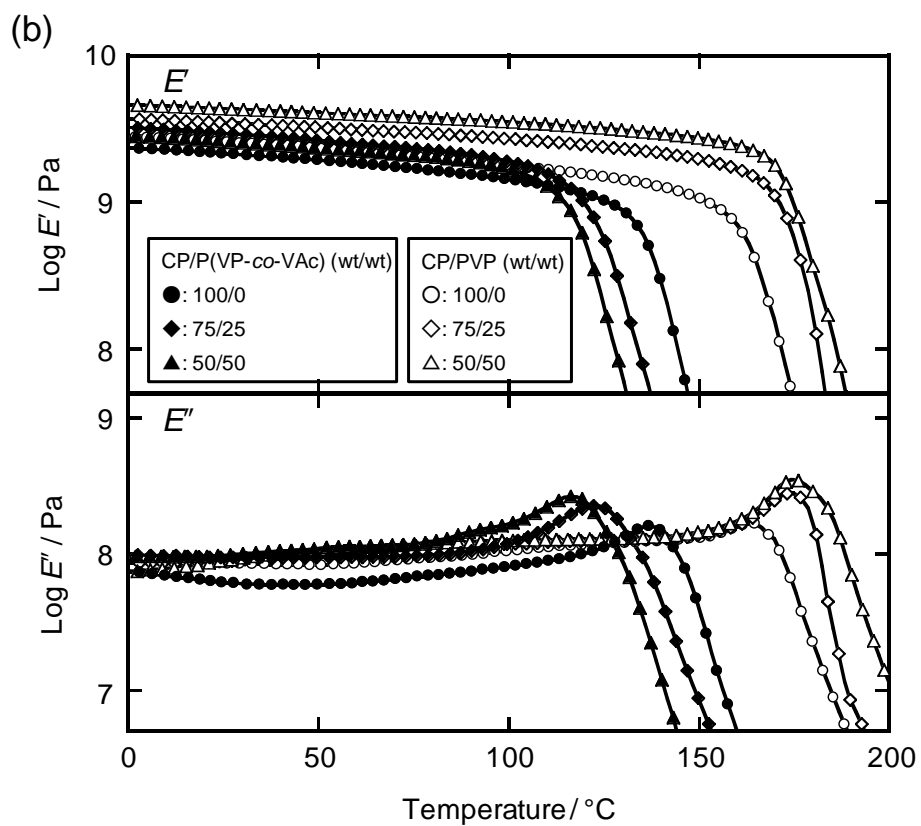
624 fraction in P(VP-co-VAc). Symbols indicate that a given pair of CP/P(VP-co-VAc) is

625 miscible (○), immiscible (×), or partially miscible (△).

626



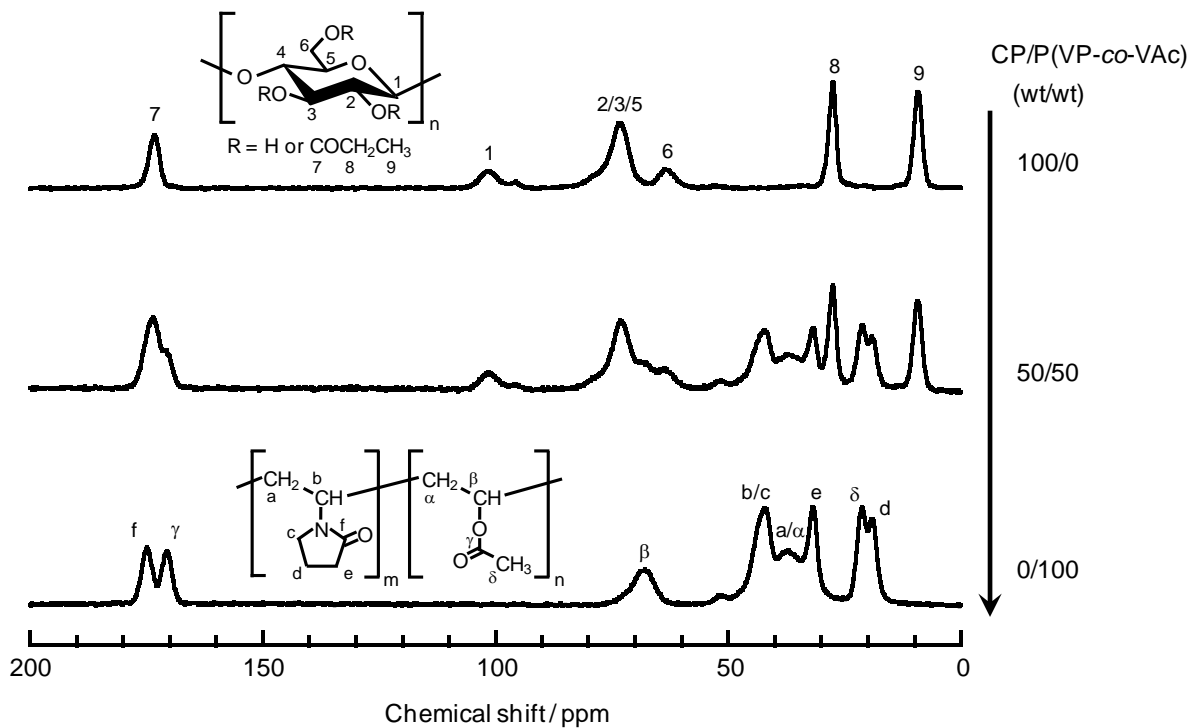
627



628

629 **Fig. 8** Temperature dependence of the dynamic storage modulus E' and loss modulus E'' for

630 (a) CP_{2.89}/P(VP_{0.10}-co-VAc_{0.90}) and (b) CP_{2.18}/PVP and CP_{2.89}/P(VP_{0.52}-co-VAc_{0.48}) blends.



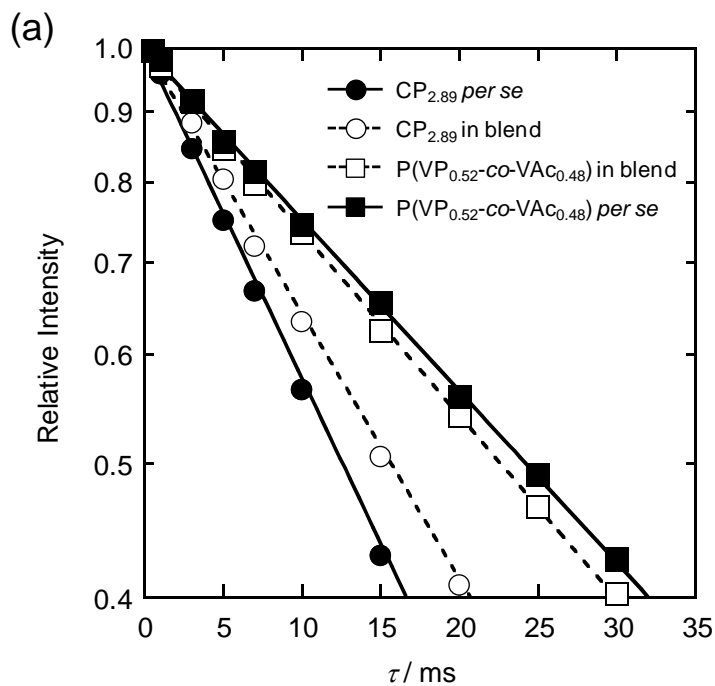
631

632

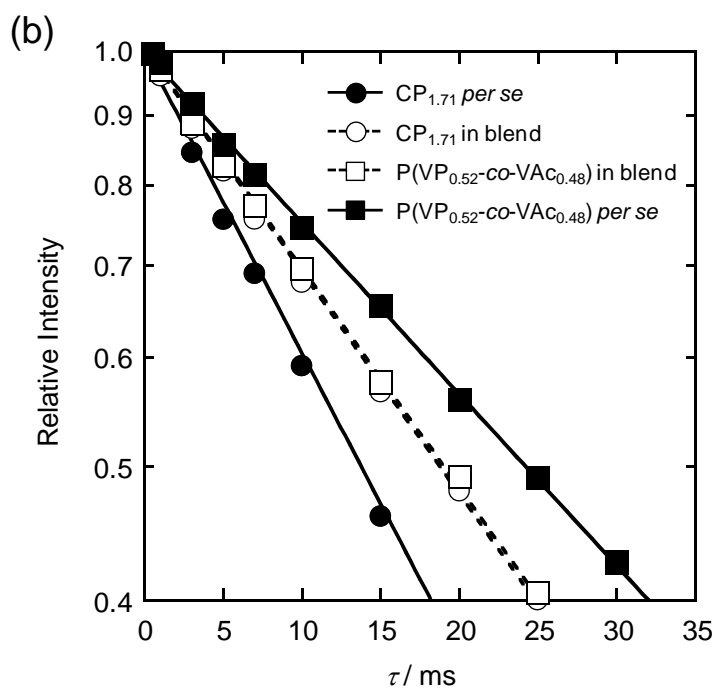
633 **Fig. 9** Solid-state ^{13}C CP/MAS NMR spectra for $\text{CP}_{2.89}$, $\text{P}(\text{VP}_{0.52}\text{-co-VAc}_{0.48})$, and their

634 50/50 blend.

635



636



637

638

639 **Fig. 10** Semilogarithmic plots of the decay of ^{13}C resonance intensities as a function of
 640 spin-locking time τ , for solid films of (a) CP_{2.89}, P(VP_{0.52-co-VAc}_{0.48}), and their 50/50 blend,
 641 and (b) CP_{1.71}, P(VP_{0.52-co-VAc}_{0.48}), and their 50/50 blend. The monitoring was conducted
 642 for the peak intensity of C2/C3/C5 pyranose carbons of CP and that of C_b/C_c carbons of the
 643 copolymer (see Fig. 9).